Mechanistic Studies of Protein Tyrosine Phosphatases YopH and Cdc25A with *m*-Nitrobenzyl Phosphate†

Daniel F. McCain,‡,§ Piotr K. Grzyska,§,|| Li Wu,⊥ Alvan C. Hengge,*,|| and Zhong-Yin Zhang*,‡,⊥

Departments of Biochemistry and Molecular Pharmacology, Albert Einstein College of Medicine, 1300 Morris Park Avenue, Bronx, New York 10461, and Department of Chemistry and Biochemistry, Utah State University, Logan, Utah 84322

Received February 23, 2004; Revised Manuscript Received May 3, 2004

ABSTRACT: Protein tyrosine phosphatases (PTPs) constitute a large family of signaling enzymes that include both tyrosine specific and dual-specificity phosphatases that hydrolyze pSer/Thr in addition to pTyr. Previous mechanistic studies of PTPs have relied on the highly activated substrate *p*-nitrophenyl phosphate (*p*NPP), an aryl phosphate with a leaving group pK_a of 7. In the study presented here, we employ *m*-nitrobenzyl phosphate (*m*NBP), an alkyl phosphate with a leaving group pK_a of 14.9, which mimics the physiological substrates of the PTPs. We have carried out pH dependence and kinetic isotope effect measurements to characterize the mechanism of two important members of the PTP superfamily: *Yersinia* PTP (YopH) and Cdc25A. Both YopH and Cdc25A exhibit bell-shaped pH−rate profiles for the hydrolysis of *m*NBP, consistent with general acid catalysis. The slightly inverse $^{18}(V/K)_{nonbridge}$ isotope effects (0.9999 for YopH and 0.9983 for Cdc25A) indicate a loose transition state with little nucleophilic participation for both enzymes. The smaller $^{18}(V/K)_{bridge}$ primary isotope effects (0.9995 for YopH and 1.0012 for Cdc25A) relative to the corresponding isotope effects for *p*NPP hydrolysis suggest that protonation of the leaving group oxygen at the transition state by the general acid is ahead of P−O bond fission with the alkyl substrate, while general acid catalysis of *p*NPP by YopH is more synchronous with P−O bond fission. The isotope effect data also confirm findings from previous studies that Cdc25A utilizes general acid catalysis for substrates with a leaving group pK_a of >8, but not for *p*NPP. Interestingly, the difference in the kinetic isotope effects for the reactions of aryl phosphate *p*NPP and alkyl phosphate *m*NBP by the PTPs parallels what is observed in the uncatalyzed reactions of their monoanions. In these reactions, the leaving group is protonated in the transition state, as is the case in PTP-catalyzed reactions. Also, the phosphoryl group in the transition states of the enzymatic reactions does not differ substantially from those of the uncatalyzed reactions. These results provide further evidence that these enzymes do not change the transition state but simply stabilize it.

Protein phosphorylation has evolved as one of the most important and versatile cell signaling mechanisms in eukaryotic organisms. Thus, phosphoryl transfer is one of the most prevalent and fundamental biochemical reactions. The addition of a phosphoryl group to the hydroxyl of a serine, threonine, or tyrosine residue can drastically alter the properties of a protein by adding two negative charges and several potential hydrogen bonding sites. This can serve to activate, inhibit, or alter the binding sites of enzymes or other proteins, thus up- or downregulating signaling pathways. Transfer of the γ-phosphoryl group from ATP to protein hydroxyl groups, forming protein phosphate monoesters, is catalyzed by protein kinases, an important class of enzymes widely recognized as the workhorses of cell signaling. Phosphate esters are intrinsically very stable, having half-lives on the order of 10^{12} years in the absence of catalysts (*1*). Therefore, the hydrolysis of phosphoamino acids on a physiological time scale requires highly potent enzymes, called protein phosphatases. Though originally considered housekeeping enzymes that serve to nonspecifically reverse the actions of the kinases, protein phosphatases are now known to play pivotal roles in cell signaling and rival the kinases in their diversity and substrate specificities.

One important class of protein phosphatases consists of the protein tyrosine phosphatases (PTPs), of which there are approximately 100 encoded in the human genome. Unlike protein kinases, in which the sequences of tyrosine specific and serine/threonine specific kinases are somewhat identical, the PTPs show no sequence similarity with serine/threonine phosphatases, or the broad specificity phosphatases such as acid or alkaline phosphatases (*2*). The hallmark that defines the PTP superfamily is the active site amino acid sequence **C**$(X)_5$**R**(S/T), also called the PTP signature motif, in the catalytic domain. PTPs include the tyrosine specific and the dual-specificity phosphatases, which are capable of hydrolyzing pSer/pThr as well as pTyr residues. Until recently, our

† This work was supported by National Institutes of Health Grants CA69202, GM47298, and 1U54 AI057158 and the G. Harold and Leila Y. Mathers Charitable Foundation.

* To whom correspondence should be addressed. A.C.H.: telephone, (435) 797-3442; fax, (435) 797-3390; e-mail, hengge@cc.usu.edu. Z.-Y.Z.: telephone, (718) 430-4288; fax, (718) 430-8922; e-mail, zyzhang@aecom.yu.edu.

‡ Department of Biochemistry, Albert Einstein College of Medicine.

§ These authors contributed equally to this work.

|| Utah State University.

⊥ Department of Molecular Pharmacology, Albert Einstein College of Medicine.

10.1021/bi0496182 CCC: $27.50
Published on Web 06/03/2004

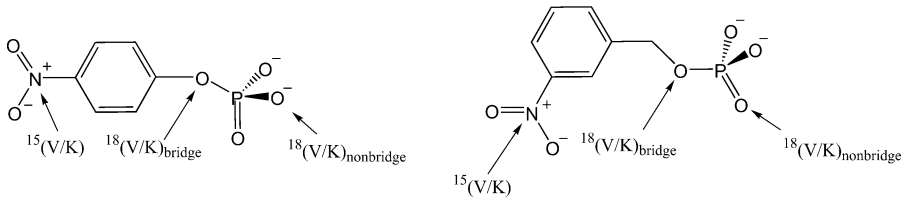

*p*NPP *m*NBP

FIGURE 1: Structures and isotope effects for *p*NPP (left) and *m*NBP (right).

understanding of PTP catalysis has been derived primarily from studies with small molecule aryl phosphates, such as *p*-nitrophenyl phosphate (*p*NPP). Since the reactions with small molecule substrates are in general slower than those with physiological ones, chemistry in most cases is the rate-limiting step. Thus, the use of low-molecular weight substrates has enabled the determination of the kinetic and chemical mechanism of the PTP reaction, the elucidation of essential residues in PTP catalysis, and a full characterization of the transition state of the PTP-catalyzed reaction (*2*).

Kinetic isotope effect studies have been particularly useful in characterizing the transition state and mechanism of PTPs (*3*−*7*). In all of these studies, the isotopically labeled substrate used was *p*NPP, shown to the left in Figure 1. Though these studies have been valuable in providing information about the mechanism of these enzymes, they suffer from the fact that *p*NPP is intrinsically 10000-fold more reactive than pTyr [based on the large $\beta_{\text{leaving group}}$ value of −1.23 for the uncatalyzed reaction (*8*)] and at least 10^6-fold more reactive than pSer and pThr, the physiological substrates of dual-specificity phosphatases. Therefore, the mechanism for *p*NPP hydrolysis may not reflect the true mechanism for the hydrolysis of the much less reactive physiological substrates. This was particularly highlighted by studies of the Cdc25A phosphatase for which it was shown that hydrolysis of low-leaving group pK_a substrates, such as *p*NPP, proceeds via a mechanism different from that of high-leaving group pK_a substrates (*7*).

A critical gap in our understanding of the PTP mechanism and transition state has been the absence of kinetic isotope effects with a substrate with a leaving group pK_a value in the physiological range of 10−16. Such an isotopically labeled substrate was simply not available before. Fortunately, we have been able to synthesize isotopically labeled *m*-nitrobenzyl phosphate (*m*NBP) (*9*), shown at the right in Figure 1, which has a leaving group pK_a of 14.9. *m*NBP has several features which make it a valuable mechanistic probe for protein phosphatases. Its leaving group pK_a value is closer to those of the physiological substrates of protein phosphatases. It is an alkyl phosphate like pSer and pThr residues, which are the physiological substrates of dual-specificity phosphatases. It also has a phenyl ring which makes it sterically similar to pTyr. In fact, we have shown previously that similar alkyl phosphates that contain an adjacent aromatic system, such as pyridoxal 5′-phosphate, serve as substrates for both tyrosine specific PTPs and dual-specificity phosphatases (*10*, *11*).

In this study, we show that *m*NBP could serve as a substrate for tyrosine specific as well as the dual-specificity phosphatases. We report the first application of this substrate in determining the kinetic isotope effects for phosphatase enzymes. Specifically, we chose to study the *Yersinia* PTP (YopH) and Cdc25A. YopH is an essential virulence determinant of *Yersinia pestis*, the causative agent of bubonic plague (*12*). In addition, YopH is the best characterized PTP, and it serves as a model system for the entire PTP family (*2*). YopH has been shown to employ general acid catalysis with *p*NPP as well as higher-leaving group pK_a substrates (*3*, *13*, *14*). Therefore, the isotope effects measured with *m*NBP will provide a benchmark for the isotope effects expected for hydrolysis of this substrate by a PTP in which general acid catalysis is known to be operating. The dual-specificity phosphatase Cdc25A is an activator of cell cycle progression, and a potential target for cancer chemotherapy. It was shown previously that Cdc25A hydrolyzes *p*NPP and other low-leaving group pK_a substrates without the use of a general acid, but it appeared that Cdc25A does employ a general acid in the hydrolysis of substrates with a leaving group pK_a of >8 (*7*). Thus, isotope effect measurements for the hydrolysis of *m*NBP by Cdc25A should allow us to more directly assess the requirement of general acid catalysis for this enzyme. In performing these studies, we reveal several important findings, namely, that Cdc25A does utilize general acid catalysis when presented with a high-leaving group pK_a substrate and that transition states for *m*NBP hydrolysis by the PTPs are characterized by less advanced phosphoester bond cleavage than for the corresponding *p*NPP transition state and full protonation of the leaving group.

EXPERIMENTAL PROCEDURES

Materials. *p*-Nitrophenyl phosphate (*p*NPP) was obtained from Sigma. Alkaline phosphatase from chicken spleen was purchased from Sigma. Diethyl ether was used as purchased. The bis(cyclohexylammonium) salt of natural abundance and isotopically labeled *m*-nitrobenzyl phosphate (*m*NBP) were synthesized as previously described (*9*). The *Yersinia* PTP YopH and its general acid mutant D356N were expressed and purified as described previously (*13*, *15*). Cdc25A and the E431Q mutant were purified as described previously (*7*) except that bacterial cells were resuspended and lysed by incubation with 200 μg/mL lysozyme, 10 μg/mL RNAse A, and 5 μg/mL DNAse on ice for 30 min followed by sonication. Additionally, the gel filtration step was carried out on an S-75 FPLC column and run on an AKTA purifier at 4 °C instead of on a conventional gravity column. The time required for this step was reduced to hours rather than days and resulted in a higher-activity protein.

Enzyme Assay and pH Dependence Studies. Enzyme kinetic assays were carried out as described previously (*7*, *14*). The following buffers were used: 100 mM acetate for pH 4.0−5.5, 100 mM succinate for pH 5.5−5.8, 50 mM 3,3-dimethyl glutarate for pH 5.8−7.2, and 50 mM Tricine for

pH 7.2−8.4. The ionic strength of each buffer was adjusted to 150 mM by the addition of sodium chloride. Additionally, each buffer contained 1 mM EDTA. All of the assays were performed at 30 °C. For the YopH-catalyzed hydrolysis of *m*NBP, assay mixtures 50 μL in total volume were set up in 96-well plates. Reactions were started by the addition of an appropriate amount of YopH (25 μL) to 25 μL of solutions containing various concentrations of *m*NBP. The reactions were quenched with 10% trichloroacetic acid (25 μL), and the amount of inorganic phosphate released was quantitated using the method of Black and Jones (*16*). The only differences were that 62 μL of the ammonium molybdate/ascorbic acid solution was added to each quenched reaction mixture followed 2−5 min later by 125 μL of the citrate/arsenite solution. The absorbance at 700 nm was read using a Spectra Max 340 plate reader from Molecular Devices. The steady state kinetic parameters were determined from a direct fit of the initial rate versus substrate concentration data to the Michaelis−Menten equation using the nonlinear regression program KINETASYST (IntelliKinetics, State College, PA).

For Cdc25A, 100 μL reactions were set up in 1.1 mL polypropylene tubes from Marsh Biomedical and allowed to equilibrate in a 30 °C water bath. A 100 μM solution of Cdc25A in 10 mM DTT, 25 mM HEPES (pH 7.4), and 200 mM sodium chloride was incubated on ice for approximately 30 min or more prior to the assay. Each reaction was initiated with the addition of enzyme to a final concentration of 5 μM. For the substrates *m*NBP, 4-chlorophenyl phosphate, and phenyl phosphate, a modified inorganic phosphate detection procedure was used to determine the amount of phosphate released during each enzymatic reaction. Each reaction was quenched with 50 μL of 10% trichloroacetic acid, and the amount of inorganic phosphate released was quantitated using the method of Black and Jones (*16*). The only differences were that 100 μL of the ammonium molybdate/ascorbic acid solution was added to each quenched reaction mixture followed 2−5 min later by 200 μL of the citrate/arsenite solution. Two hundred microliters of each reaction mixture was then transferred to a 96-well plate, where the absorbance at 700 nm was read using a Spectra Max 340 plate reader from Molecular Devices. As some of these substrates are only soluble to 5−10 mM, sufficient substrate could not be added to saturate Cdc25A. Therefore, k_{cat}/K_m values were determined by employing a series of assay solutions containing a range of substrate concentrations (0.3−1.7 mM) well below the K_m. The k_{cat}/K_m values were obtained from a linear least-squares fit of the plot of absorbance versus substrate concentration and using the appropriate form of the Michaelis−Menten equation

$$v = k_{cat}[E][S]/K_m \quad (1)$$

where v is the initial rate and [E] is the total enzyme concentration. The k_{cat}/K_m versus pH data were fit to one of the following equations using Kaleidagraph:

$$k_{cat}/K_m = (k_{cat}/K_m{}^{max})/(1 + H/K_1 + K_2/H) \quad (2)$$

$$k_{cat}/K_m = (k_{cat}/K_m{}^{max})/[(1 + H/K_1)(1 + K_2/H)] \quad (3)$$

$$k_{cat}/K_m = (k_{cat}/K_m{}^{max})/[(1 + H/K_1)(1 + H/K_2 + K_3/H)] \quad (4)$$

where K_1−K_3 are the apparent acid dissociation constants of the enzyme and/or substrate and H is the proton concentration.

Isotope Effect Determinations. ^{18}O kinetic isotope effects were measured using isotope ratio mass spectrometry by the remote label method, using the nitrogen atom as a reporter for isotopic fractionation at the bridge or nonbridge oxygen atoms. The experimental procedures used to measure these isotope effects were similar to those previously reported in earlier papers (*17*). The isotopic isomers of *m*NBP (*9*) used for measurement of kinetic isotope effects are shown below:

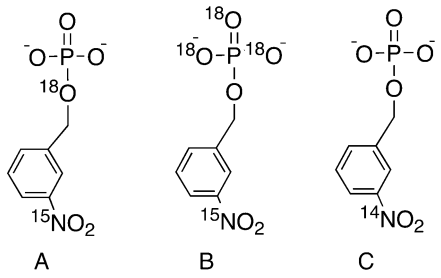

A mixture of isotopic isomers A and C was used to determine $^{18}(V/K)_{bridge}$. Isomers B and C were also mixed to reconstitute the natural abundance of ^{15}N and used to determine $^{18}(V/K)_{nonbridge}$. The isotopic abundance of the mixtures was determined by isotope ratio mass spectrometry. The unlabeled compound, containing the natural abundance of ^{15}N, was used to measure the ^{15}N isotope effect.

Cdc25A isotope effect experiments were conducted at pH 6.0 using 0.2 M BisTris buffer containing 1 mM DTT. A temperature of 30 °C was maintained with a thermostated heating block. The dicyclohexylammonium salt (43 mg) of the appropriate isotopically labeled form of the substrate was dissolved in 10 mL of buffer that had been flushed with nitrogen for 30 min before reaction. Reactions were initiated by addition of 300−450 μL of enzyme (260−290 μM). Since these reactions are slow, sufficient enzyme was used to give a half-life for reaction of ∼48 h. Reactions were run in duplicate or triplicate and were allowed to progress for varying times to obtain fractions of reaction varying from approximately 20 to 50%. Reactions were monitored by ^{31}P NMR, and control experiments carried out under the same conditions without enzyme exhibited no measurable substrate hydrolysis.

Wild-type YopH isotope effect experiments were carried out at pH 6.0 and 7.60 using 0.2 M BisTris buffer containing 1 mM DTT at 30 °C. The dicyclohexylammonium salt (43 mg) of the appropriate isotopically labeled form of *m*NBP was dissolved in 10 mL of buffer that had been flushed with nitrogen for 30 min before reaction. Reactions were initiated by addition of 250 μL of enzyme (∼2 mg/mL lyophilized YopH) and were monitored by ^{31}P NMR.

After partial hydrolysis, reaction mixtures were extracted with diethyl ether four times (25 mL) to separate the product, *m*-nitrobenzyl alcohol. These ether layers were dried over magnesium sulfate, and the ether was removed by rotary evaporation. The *m*-nitrobenzyl alcohol was further purified by distillation at ∼105 °C onto a coldfinger apparatus before isotopic analysis by isotope ratio mass spectrometry using an ANCA-NT combustion system working in tandem with a Europa 20-20 isotope ratio mass spectrometer. The aqueous

layer, containing the unreacted *m*NBP, was added to Tris buffer containing 1 mM Zn^{2+} and 1 mM Mg^{2+}, and were titrated to pH ~9. Approximately 1 mg of commercially available alkaline phosphatase was added to cleave the residual *m*NBP. After more than 10 half-lives, this mixture was treated as described above to recover *m*-nitrobenzyl alcohol.

Isotope effects were calculated from the nitrogen isotopic ratios at partial reaction in the product (R_p), in the residual substrate (R_s), and in the starting material (R_o).

$$\mathrm{KIE} = [\log(1 - f)]/\{\log[1 - f(R_p/R_o)]\} \quad (5)$$

$$\mathrm{KIE} = [\log(1 - f)]/\{\log[(1 - f)(R_s/R_o)]\} \quad (6)$$

Equation 5 or 6 was used to calculate the observed isotope effect either from R_p and R_o or from R_s and R_o, respectively, at the fraction of reaction. Experiments using the natural abundance compound showed there is no measurable ^{15}N isotope effect. The ^{18}O isotope effects were corrected for levels of isotopic incorporation, as previously described. The independent calculation of each isotope effect using R_o and R_p and using R_o and R_s from eqs 5 and 6, respectively, provides an internal check of the results.

RESULTS AND DISCUSSION

Extensive biochemical and mechanistic studies have shown that members of the PTP family utilize a common mechanism to effect catalysis (*2*). In this mechanism, PTPs employ covalent catalysis, utilizing the thiol group of the active site cysteine (Cys403 in YopH) as the attacking nucleophile, to form a thiophosphoryl enzyme intermediate (E−P) (*18*, *19*). In the first catalytic step, E−P formation is assisted by a conserved aspartic acid (Asp356 in YopH), functioning as a general acid, to neutralize the buildup of a negative charge on the leaving group (*3*, *13*, *20*). In the second step, the hydrolysis of E−P occurs by the attack of a nucleophilic water molecule assisted by Asp356, which functions as a general base, with subsequent release of the free enzyme and inorganic phosphate. The PTPs further accelerate the formation and hydrolysis of E−P by preferentially binding the pentacoordinated transition states with the guanidinium side chain of the active site arginine (Arg409 in YopH) (*21*−*23*).

Isotope effects have been very useful in characterizing the transition state and general acid catalysis for PTPs such as *Yersinia* PTP and PTP1B (*3*), the low-molecular weight PTP Stp1 (*5*), and the dual-specificity phosphatases VHR (*4*), MKP3 (*6*), and Cdc25A (*7*). In all cases, the kinetic isotope effects with *p*NPP as a substrate reveal a loose transition state for PTP catalysis. Additionally, they reveal the presence of general acid catalysis for the *p*NPP substrate for all of the aforementioned enzymes, except Cdc25A. The substrate *p*NPP has a leaving group pK_a value of 7.1, much lower than those of the physiological substrates pTyr (10.5) and pSer and pThr (13−16). Despite this difference, for the PTPs studied so far, only in the case of Cdc25A is there evidence that *p*NPP is hydrolyzed via a mechanism significantly different from that of pTyr, pSer, or pThr (*7*). However, for any of these phosphatases, the structure of the transition state may differ with a less reactive substrate. *m*NBP is an alkyl phosphate with a leaving group pK_a value in the more physiologically relevant range of 13−16, and it provides the opportunity to gain valuable insights into the PTP transition state.

Previously, we showed, using kinetic isotope effects with *p*NPP, mutagenesis, and pH dependence studies with *p*NPP and other aryl phosphates, that the *Yersinia* PTP YopH employs general acid catalysis when hydrolyzing these substrates, and identified the general acid as Asp356 (*3*, *13*). On the basis of results from kinetic isotope effects and pH dependence studies, we showed that Cdc25A does not employ general acid catalysis in the hydrolysis of *p*NPP (*7*). Interestingly, our pH dependence and leaving group dependence data using other aryl phosphates suggested that Cdc25A could employ general acid catalysis for substrates with a leaving group pK_a of >8. We suggested that there are two competing mechanisms, general acid catalysis and general acid-independent catalysis, by which the substrate can react. For the more reactive substrates (those with leaving group pK_a values of <8), the general acid independent route was much faster and is the only mechanism that is observed. For the less reactive substrates, with leaving group pK_a values of >8, the general acid-independent route was so slow that the competing process, general acid catalysis, dominates. The synthesis of natural abundance and isotopically labeled *m*NBP, which has a leaving group pK_a value of 14.9 (*24*), enables the first comprehensive kinetic and isotope effect study of PTPs using a substrate with a leaving group pK_a value in the physiologically relevant range.

mNBP Is a Substrate for YopH and Cdc25A. Before kinetic isotope effects could be measured with *m*NBP, we first needed to determine whether *m*NBP could serve as a substrate for YopH and Cdc25A. Because Cdc25A is a dual-specificity phosphatase, able to hydrolyze pSer and pThr as well as pTyr, it is expected to be able to hydrolyze an alkyl phosphate such as *m*NBP. However, Cdc25A is known to have rather low activity except when presented with its physiological substrate (*25*), so it is important to determine the kinetic parameters of the Cdc25A-catalyzed hydrolysis of *m*NBP. Though tyrosine specific PTPs such as YopH are specifically designed for optimal hydrolysis of aryl phosphates, they also display limited activity against alkyl phosphates (*10*, *26*). The activity of PTPs toward alkyl phosphates could be significantly augmented if an aromatic moiety is attached to the alkyl phosphate (*10*). For example, pyridoxal 5′-phosphate and flavin mononucleotide are substantially better substrates for PTPs than simple alkyl phosphates, including pSer and pThr. Given the importance of aromatic moieties in PTP binding and the fact that the phenyl group of *m*NBP makes it sterically similar to pTyr, it is expected that YopH will be able to hydrolyze *m*NBP. Indeed, both YopH and Cdc25A were able to hydrolyze *m*NBP as measured by the production of inorganic phosphate. As expected, the kinetic parameters for *m*NBP hydrolysis are similar to those of pyridoxal 5′-phosphate (*10*). As shown in Table 1, the k_{cat} values for the YopH-catalyzed hydrolysis of *m*NBP are 2 orders of magnitude lower than those of *p*NPP, while the K_m values for *m*NBP and *p*NPP are similar. The decrease in k_{cat} for the hydrolysis of *m*NBP may result from a change in the rate-limiting step from E−P hydrolysis for aryl phosphates to E−P formation for alkyl substrates. For Cdc25A, the k_{cat}/K_m for *m*NBP is only 3-fold lower than that of *p*NPP (Table 2).

Table 1: Kinetic Parameters of YopH[a]

		pH 5.0		pH 6.0		pH 7.0	
	substrate	k_{cat} (s^{-1})	K_m (mM)	k_{cat} (s^{-1})	K_m (mM)	k_{cat} (s^{-1})	K_m (mM)
wild type	*p*NPP	1230 ± 39	2.55 ± 0.17	345 ± 5.5	2.60 ± 0.12	34.2 ± 2.6	2.90 ± 0.52
wild type	*m*NBP	4.97 ± 0.35	4.86 ± 0.20	3.36 ± 0.18	4.20 ± 0.12	0.72 ± 0.07	2.60 ± 0.08
D356N	*p*NPP	0.72 ± 0.02	3.65 ± 0.23	0.89 ± 0.02	3.38 ± 0.20	0.89 ± 0.04	3.28 ± 0.30
D356N	*m*NBP			0.0052 ± 0.0003	5.0 ± 0.5		

[a] All assays were carried out at 30 °C as described in Experimental Procedures.

Table 2: Kinetic Parameters of Cdc25A[a]

	substrate	k_{cat}/K_m at pH 7 (M^{-1} s^{-1})
wild type	*p*NPP	22.6 ± 1.4
wild type	*m*NBP	7.9 ± 0.3
E431Q	*p*NPP	60.1 ± 5.7
E431Q	*m*NBP	<0.1

[a] All assays were carried out at 30 °C as described in Experimental Procedures.

pH Dependence of mNBP Hydrolysis by YopH and Cdc25A. Before measuring isotope effects, we also wanted to show that *m*NBP behaves as expected on the basis of our previous studies employing aryl substrates for these two enzymes. The kinetic parameter k_{cat}/K_m monitors the reaction beginning with binding of the substrate up to and including the first irreversible step in the kinetic mechanism, which is E−P formation accompanied by release of the leaving group. Previously, it was shown for YopH that the hydrolysis of *p*NPP followed a bell-shaped k_{cat}/K_m versus pH profile with a slope of 2 on the acidic side and a slope of −1 on the basic side (*14*). This indicates that three ionizations of the free enzyme and/or free substrate are involved in the reaction of *p*NPP. Fitting the data to eq 4 yielded values of 5.1, 3.3, and 5.1 for pK_1, pK_2, and pK_3, respectively, for the reaction of YopH with *p*NPP. Values of 5.5, 3.4, and 5.1 were obtained for pK_1, pK_2, and pK_3, respectively, for the reaction of YopH with β-naphthyl phosphate (*14*). An excellent correspondence was found between the values of pK_1 and the values of the second ionization constant of the phosphate substrates measured by titration (5.1 for *p*NPP and 5.5 for β-naphthyl phosphate). Therefore, it was concluded that the apparent pK_1 was caused by the deprotonation of the substrate and that the dianionic form of the substrate was the form that was hydrolyzed by YopH. Similar conclusions have been generated by studies of PTP1B and the dual-specificity phosphatase VHR (*20*, *27*). That the dianionic form of the substrate is the form recognized by PTPs has been supported by computational studies (*28*, *29*). The pK_3 value of 5.1 has been attributed to an enzyme residue that must be protonated for catalysis to occur, the general acid, Asp356 (*3*, *13*). The ability of Asp356 to act as a general acid is also supported by both structural and mutagenesis data (*2*).

Within this framework, we expect that the substrate *m*NBP should follow a similar k_{cat}/K_m versus pH profile, with pK_1 corresponding to the second ionization constant of *m*NBP. This is indeed what we observe as shown in Figure 2. The acidic limb has a slope of 2 and the basic limb a slope of −1, as expected. Values of 6.3 ± 0.1, 3.8 ± 0.4, and 5.0 ± 0.4 were obtained for pK_1, pK_2, and pK_3, respectively, by fitting the data to eq 4. The pK_2 and pK_3 values are in excellent agreement with those determined from the pH dependence of the YopH-catalyzed hydrolysis of *p*NPP and

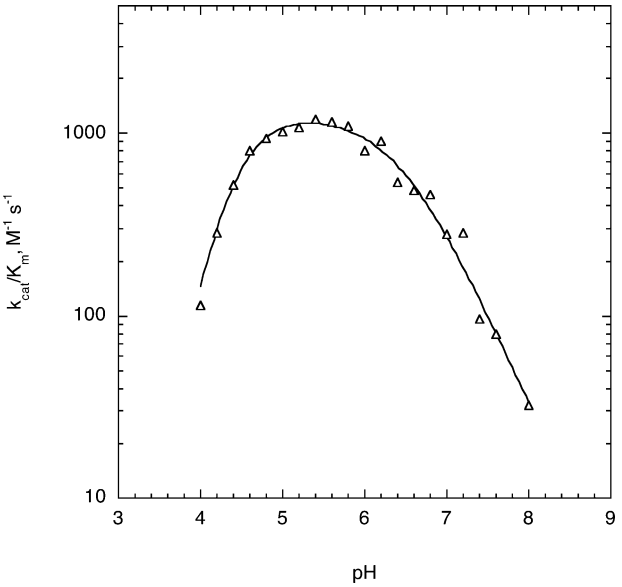

FIGURE 2: pH dependence of k_{cat}/K_m for YopH using *m*NBP. The solid line was generated by fitting the data to eq 4.

β-naphthyl phosphate. The value of 6.3 obtained for pK_1 correlates well with the second ionization constant of 6.2 measured for *m*NBP by NMR (*9*). Therefore, we can conclude that, as for *p*NPP and β-naphthyl phosphate, YopH hydrolyzes the dianion of *m*NBP and employs general acid catalysis to do so. In support of this, a 650-fold decrease in k_{cat} was observed for *m*NBP hydrolysis by the general acid deficient mutant D356N (Table 1). A similar drop in k_{cat} was also observed for D356N-catalyzed *p*NPP hydrolysis.

Likewise for Cdc25A, we also needed to show that the general conclusions reached in our previous study (*7*) can be applied to the substrate *m*NBP before we can proceed to characterize the transition state in which general acid catalysis is involved. On the basis of this previous work, we would predict that *m*NBP, having a leaving group pK_a value of >8 (pK_a = 14.9), should exhibit a pH dependence similar to that of the other small molecule high-leaving group pK_a substrates. As Figure 3 shows, this is indeed what we observe. Figure 3 shows the pH dependence of the k_{cat}/K_m for *m*NBP (△) along with 4-chlorophenyl phosphate (○) and phenyl phosphate (□) for comparison. As for 4-chlorophenyl phosphate and phenyl phosphate, *m*NBP exhibits a bell-shaped pH profile with a maximum at pH 6 in its hydrolysis by Cdc25A. This suggests that like the other high-leaving group pK_a substrates that have been examined, *m*NBP also requires protonation of a residue on Cdc25A for efficient hydrolysis. We would also predict that mutation of Glu431, the putative general acid of Cdc25A identified in our previous study (*7*), into glutamine should abolish the ability of Cdc25A to hydrolyze *m*NBP. In fact, the E431Q mutant of Cdc25A displays no measurable activity against *m*NBP

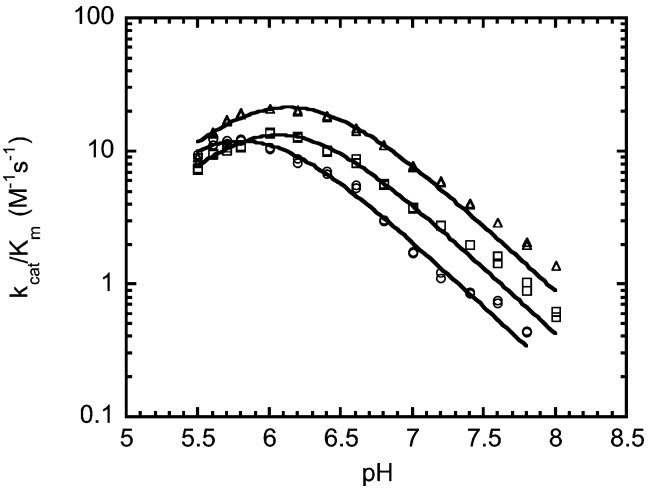

FIGURE 3: pH dependence of k_{cat}/K_m for Cdc25A using the substrates 4-chlorophenyl phosphate (○), phenyl phosphate (□), and *m*NBP (△). The curves were fit to eq 2.

(Table 2, data not shown). This suggests that, like all other substrates with leaving group pK_a values of >8 that have been examined, Glu431 is required for efficient hydrolysis of *m*NBP. In contrast, the Cdc25A-catalyzed hydrolysis of *p*NPP exhibits no pH dependence, and the kinetic parameters for the E431Q-catalyzed *p*NPP reaction are similar to those of wild-type Cdc25A (*7*).

Expected Contributions to Isotope Effects with mNBP Compared to Those with pNPP. ^{18}O isotope effects were measured in the bridging position [designated $^{18}(V/K)_{bridge}$] and nonbridging positions [$^{18}(V/K)_{nonbridge}$]. The primary $^{18}(V/K)_{bridge}$ isotope effect is the product of the normal isotope effect arising from P−O bond fission, and the inverse isotope effect from protonation. The ^{18}O isotope effect on phosphoryl transfer is larger than that for proton transfer, because of the bending and torsional modes present in the phosphate ester but absent when the phosphoryl group is replaced with a proton. P−O bond fission in *p*NPP results in a maximum value of ~1.03 (3% normal), while the equilibrium isotope effect (EIE) for protonation of *p*-nitrophenolate ion is 0.985 (1.5% inverse).[1] The trend of $^{18}(V/K)_{bridge}$ in prior studies with PTPs shows that the maximal value for this KIE is observed when protonation is eliminated by removal of the general acid, and $^{18}(V/K)_{bridge}$ is reduced by ~1.5% in the native enzymes where LFER studies indicate the leaving group is fully neutralized (*3*−*5*, *30*). Intermediate values are observed when mutations result in less efficient, but still partial, protonation of the leaving group in the transition state (*23*, *31*). The fact that the normal isotope effect for full dephosphorylation is larger than the inverse contribution for full protonation is the relevant fact for interpretation of the $^{18}(V/K)_{bridge}$ isotope effects presented below.

The $^{18}(V/K)_{nonbridge}$ isotope effect reflects the degree of nucleophilic participation in the transition state (*32*). A loose transition state, in which leaving group bond fission exceeds bond formation to the nucleophile, is characterized by a small inverse $^{18}(V/K)_{nonbridge}$ isotope effect. A tight mechanism, on the other hand, in which bonding of the attacking nucleophile and the departing leaving group to the phosphorus atom are both substantial, results in a normal $^{18}(V/K)_{nonbridge}$ isotope effect due to the decreased bond order between the nonbridging oxygens and the phosphorus atom.

With the *p*-nitrophenol leaving group, a normal $^{15}(V/K)$ accompanies charge delocalization into the nitrophenolate ring, a result of contribution of a quinonoid resonance structure. With *m*-nitrobenzyl alcohol, no such participation of the aromatic ring is possible, and no significant $^{15}(V/K)$ is expected in reactions with *m*NBP. In these reactions, the nitrogen atom serves as only a reporter for the nonbridging or bridging oxygen atoms.

Kinetic Isotope Effects for YopH- and Cdc25A-Catalyzed mNBP Hydrolysis. The kinetic isotope effects were determined for the hydrolysis of *m*NBP by both YopH and Cdc25A. The isotope effects for the uncatalyzed hydrolysis of the *m*NBP monoanion were recently reported (*9*). This reaction shares with both enzymatic reactions the mechanistic feature of protonation of the leaving group. Table 3 summarizes the isotope effects determined for YopH and Cdc25A, along with the corresponding isotope effects using *p*NPP as a substrate, and the isotope effects for the uncatalyzed hydrolysis reactions of *p*NPP and *m*NBP for comparison.

Isotope effects are only expressed for enzyme-catalyzed reactions when the chemical step is at least partially rate-limiting, and the formation of the enzyme−substrate complex must be freely reversible. We have shown previously that with *p*NPP as a substrate, phosphoryl transfer is rate-limiting for *V*/*K* of the PTP reaction (*3*-*7*). Since *m*NBP is an even slower substrate than *p*NPP (Tables 1 and 2), it is likely that the *V*/*K* for the PTP-catalyzed hydrolysis of *m*NBP is also rate-limited by chemistry. The fact that similar $^{18}(V/K)_{nonbridge}$ isotope effects for *m*NBP were obtained both near (pH 6) and off (pH 7.6) the pH optimum (Table 3) is consistent with chemistry being at least partially rate-limiting for the YopH reaction. For Cdc25A, we observe significant $^{18}(V/K)_{bridge}$ and $^{18}(V/K)_{nonbridge}$ isotope effects for *m*NBP hydrolysis, suggesting that chemistry is at least partially rate-limiting for Cdc25A as well. Thus, the isotope effects observed will reveal details of the phosphoryl transfer step.

YopH. The very small $\beta_{leaving\ group}$ [−0.19 (*30*)] observed for the YopH-catalyzed hydrolysis of aryl phosphates implies a minimal change in the effective charge on the aryl group in the transition state. Similarly, the $^{15}(V/K)$ of unity indicates no significant negative charge delocalized into the aromatic ring of the substrate *p*NPP in the transition state. Together, these data indicate that protonation of the leaving group cannot lag significantly behind P−O bond fission.

The primary $^{18}(V/K)_{bridge}$ isotope effect is the product of the normal isotope effect arising from P−O bond fission and

[1] The isotope effect of 3% normal cited for P−O bond fission is a kinetic isotope effect, while the 1.5% inverse isotope effect for protonation is an equilibrium effect. A kinetic isotope effect has contributions from the imaginary frequency factor, in addition to a zero-point energy difference that determines an equilibrium isotope effect, but zero-point energy is most likely the major cause of this difference in magnitude. The zero-point energy change, and hence the magnitude of the EIE, should be intrinsically larger for dephosphorylation than the EIE for deprotonation because the phosphoryl group contributes additional bending and torsional modes in the phosphate ester that are absent in the product alcohol or phenol. While no EIE for dephosphorylation has been reported, for the same reason, the EIE of 1.0277 (2.77% normal) for deacetylation (the EIE between *p*-nitrophenyl acetate and *p*-nitrophenolate ion) is larger than the EIE of 1.015 (1.5% normal) for deprotonation (the EIE between *p*-nitrophenol and *p*-nitrophenolate ion) (*38*).

Table 3: Kinetic Isotope Effects[a]

enzyme	substrate	$^{15}(V/K)$	$^{18}(V/K)_{bridge}$	$^{18}(V/K)_{nonbridge}$ observed	$^{18}(V/K)_{nonbridge}$ assuming monoanion	$^{18}(V/K)_{nonbridge}$ assuming dianion
YopH	*m*NBP, pH 6.0	0.9996 (4)	0.9995 (8)	1.0093 (3)	1.0152 (3)	0.9999 (3)
YopH	*m*NBP, pH 7.6	ND[b]	ND[b]	0.9975 (1)	1.0122 (1)	0.9970 (1)
YopH[c]	*p*NPP, pH 5.0	0.9999 (3)	1.0152 (6)	1.0073 (13)	1.0149 (13)	0.9998 (13)
Cdc25A	*m*NBP, pH 6.0	1.0002 (1)	1.0012 (3)	1.0025 (4)	1.0133 (4)	0.9983 (4)
Cdc25A[d]	*p*NPP, pH 6.1	1.0031 (4)	1.0291 (8)	ND[b]		
Cdc25A[d]	*p*NPP, pH 7.2	1.0030 (2)	1.0357 (49)	0.9988 (3)		0.9988 (3)
solution at 115 °C	*m*NBP, monoanion, pH 4.0	0.9999 (1)	0.9982 (7)	1.0149 (4)		
solution at 95 °C	*p*NPP, monoanion, pH 3.5	1.0004 (2)	1.0087 (3)	1.0184 (5)		
solution at 95 °C	*p*NPP, dianion, pH 10	1.0028 (2)	1.0189 (5)	0.9945 (2)		

[a] Isotope effects were determined at the indicated pH and 30 °C as described in Experimental Procedures. [b] Not determined. [c] From ref *3*. [d] From ref *7*.

the inverse isotope effect from protonation. The much smaller magnitude of $^{18}(V/K)_{bridge}$ with *m*NBP versus *p*NPP implies a difference in the relative progression of proton transfer and P−O bond fission. Because the inverse isotope effect from protonation is smaller than the normal contribution from P−O bond fission, the normal $^{18}(V/K)_{bridge}$ of 1.0152 (1.5%) for the hydrolysis of *p*NPP by YopH implies a late transition state in which protonation and P−O bond fission are both well-advanced, if these two processes are synchronous. An earlier transition state with respect to P−O bond fission could account for $^{18}(V/K)_{bridge}$ if protonation lags behind, but it is difficult to reconcile such a scenario with the small $\beta_{leaving\ group}$ value, and the $^{15}(V/K)$ of unity with *p*NPP. The inverse $^{18}(V/K)_{bridge}$ of 0.9995 for the hydrolysis of *m*NBP requires that the contributions from protonation and P−O bond fission essentially offset one another. This is only possible if proton transfer is ahead of P−O bond fission with the alkyl ester, in contrast to the timing between these two processes with the aryl substrate.

Cdc25A. For the Cdc25A-catalyzed *p*NPP reaction, the observed $^{18}(V/K)_{bridge}$ isotope effects (1.0291 at pH 6.1 and 1.0357 at pH 7.2) (*7*) are similar in magnitude to those of the general acid deficient PTPs (*3*−*6*) and to that found in the uncatalyzed hydrolysis of the dianion of *p*NPP (*33*). These results indicate a large degree of P−O bond cleavage without general acid catalysis. In contrast, the $^{18}(V/K)_{bridge}$ isotope effect of 1.0012 for the hydrolysis of *m*NBP by Cdc25A is greatly reduced, consistent with protonation of the leaving group oxygen by a general acid. Since mutation of Glu431 abolishes Cdc25A's ability to hydrolyze *m*NBP (Table 2) and eliminates the basic limb of the pH profile of a substrate with a leaving group pK_a value of 8 (*7*), we suggest that Glu431 is this general acid. Further, as was the case with the YopH-catalyzed reaction of *m*NBP, the value near unity means that the contributions to $^{18}(V/K)_{bridge}$ for protonation and P−O bond cleavage virtually offset one another, which requires protonation to be ahead of P−O bond fission.

In addition to distinguishing loose or tight transition states, the $^{18}(V/K)_{nonbridge}$ isotope effect is also affected by protonation. Deprotonation of phosphate monoesters is accompanied by an equilibrium $^{18}(V/K)_{nonbridge}$ isotope effect of 1.015 (*34*). At the pH values where the isotope effects were measured, a mixture of monoanion and dianion forms are present, and the nonbridge ^{16}O-labeled substrate will have a 1.5% higher proportion of the dianion form than the nonbridge ^{18}O-labeled substrate. All PTPs examined to date utilize the dianion form of the substrate, which necessitates correction of $^{18}(V/K)_{nonbridge}$ (observed) for deprotonation of the fraction of the substrate present as the monoanion. For the PTPs, some computational results have suggested the monoanion is the substrate, while other computational results, and all of the experimental results (*vide supra*), favor the dianion. For a different form of Cdc25, namely, Cdc25B, results with a phosphoprotein substrate have been interpreted to favor the monoanion substrate (*35*).

Table 3 shows the observed values of the $^{18}(V/K)_{nonbridge}$ isotope effect for the YopH- and Cdc25A-catalyzed reactions with *m*NBP along with the values corrected assuming the monoanion is the substrate, as well as the values assuming that the dianion is the substrate. The latter values are small, inverse, and very similar to those obtained for the hydrolysis of *p*NPP by these enzymes, and likewise indicate a loose transition state. The former values, assuming that the monoanion is the substrate, are normal and similar to that obtained for the solution hydrolysis of the *m*NBP monoanion. Since the hydrolyses of monoanions of phosphate monoesters, like the dianion reactions, proceed with a loose transition state (*9*, *32*, *36*, *37*), the transition state for the PTP-catalyzed hydrolysis of *m*NBP is likely loose as well, regardless of whether the monoanion or dianion is the reactive form. While the isotope effects cannot distinguish between these possibilities, other data cited previously indicate the dianion is the more likely substrate for both enzymes.

Is the Monoanion or Dianion the Substrate for Cdc25 Phosphatases? For all PTPs that have been examined, substantial evidence indicates that the dianion is the substrate as explained above. In addition to the pH dependence of k_{cat}/K_m, it has been shown that abrogation of the general acid functionality eliminates the basic limb of the pH−rate profile, and the $^{18}(V/K)_{bridge}$ and $^{18}(V/K)_{nonbridge}$ isotope effects observed for the general acid deficient mutant PTPs (*3*−*5*) are inconsistent with the monoanion as the substrate. Recently, it was proposed that for the hydrolysis of bisphosphorylated CyclinA/Cdk2pTpY by Cdc25B, the monoanionic form of pThr is the preferred substrate where the nonbridging phosphate oxygen itself acts as a general acid (*35*). If the monoanion mechanism is operative, then the basic limb of the pH profile would be produced by the second ionization constant of the substrate pK_a instead or by the deprotonation of a general acid located on Cdc25A. Unfortunately, for Cdc25A, the k_{cat}/K_m−pH dependence data (Figure 3) cannot reveal whether the preferred substrate is the monoanion or dianion, because Cdc25A is unstable at pH <5.5 such that the slope of the acidic limb cannot be determined. Addition-

ally, all of the relevant ionizations of the enzyme and substrate occur in a very narrow range from pH 5.5 to 6.2 in such a way that it is not possible to determine whether pK_2 is derived from the general acid or from the phosphate substrate itself. Nonetheless, mutational and kinetic isotope results from this study and from our previous study (*7*) strongly suggest that like other PTPs, Cdc25A utilizes Glu431 as a general acid for small molecule substrates with a leaving group pK_a of >8.

We should point out that the assumption that phosphatases prefer to use the monoanion because it is more reactive in uncatalyzed hydrolysis is based on flawed reasoning. In uncatalyzed reactions, there is no preorganized general acid, so proton transfer to the leaving group must be assisted intramolecularly. In the monoanion, a proton on the phosphoryl group is transferred (probably via an intervening solvent molecule) to the leaving group. This is what makes the monoanion more reactive than the dianion in uncatalyzed reactions. For a phosphatase with an appropriately positioned residue that can serve as this proton donor, there is no logical reason for it to use the monoanion. At this time, there is no evidence to conclude that Cdc25A utilizes the monoanionic form of small molecule substrates, particularly in light of the fact that all other PTPs employ the dianion as a substrate. Given that the k_{cat}/K_m for the reaction of Cdc25B with CyclinA/Cdk2pTpY is 6 orders of magnitude greater than those for small molecule substrates (*25*), it is possible that the mechanism is different with the protein substrate than with small molecule substrates.

Conclusions. We have kinetically characterized the hydrolysis of *m*NBP by both YopH and Cdc25A, and shown that *m*NBP exhibits some similarities and some differences compared with aryl phosphates in these enzyme-catalyzed reactions. The transition states for both enzymes, with the aryl as well as the alkyl substrate, are loose with little nucleophilic participation. For YopH, the transition state for *p*NPP hydrolysis is characterized by both extensive P−O bond cleavage and proton donation from the general acid, Asp356, to the leaving group, as shown in the top left structure of Figure 4. Protonation either is synchronous with or lags somewhat behind P−O bond fission. While the transition state for the hydrolysis of *p*NPP by Cdc25A is also characterized by extensive P−O bond cleavage, there is no proton donation by a general acid, as illustrated in the bottom left structure of Figure 4. Cdc25A employs general acid catalysis in the hydrolysis of *m*NBP, but not with *p*NPP, confirming conclusions from linear free energy relationship studies. Our pH dependence and mutagenesis studies suggest that this general acid is Glu431. Despite the structural differences between YopH and Cdc25, and the substantial differences in their transition states for *p*NPP hydrolysis, the two enzymes share very similar transition states for *m*NBP hydrolysis (Figure 4).

For both enzymes, with the alkyl substrate *m*NBP, proton transfer to the leaving group is ahead of P−O fission, in contrast to the timing of these processes in the YopH-catalyzed reaction of *p*NPP. The difference in synchronicity between proton transfer and P−O bond fission is in accord with expectations from Marcus theory. As the P−O bond begins to break, the leaving group basicity increases and protonation will become favorable when this pK_a matches that of the general acid. The pK_a of the leaving group in the alkyl ester *m*NBP will become sufficiently basic for proton transfer earlier in the reaction coordinate than *p*NPP, accounting for a greater extent of proton transfer in the transition state. Further, the similarity of the isotope effects in the enzymatic reactions with those for the uncatalyzed hydrolysis of the *m*NBP monoanion indicates similar transition states for the enzymatic and nonenzymatic processes. Finally, the data for the reaction of *m*NBP with Cdc25A confirm conclusions from Brønsted studies (*7*) that general acid catalysis accompanies the reaction of substrates with poor leaving groups.

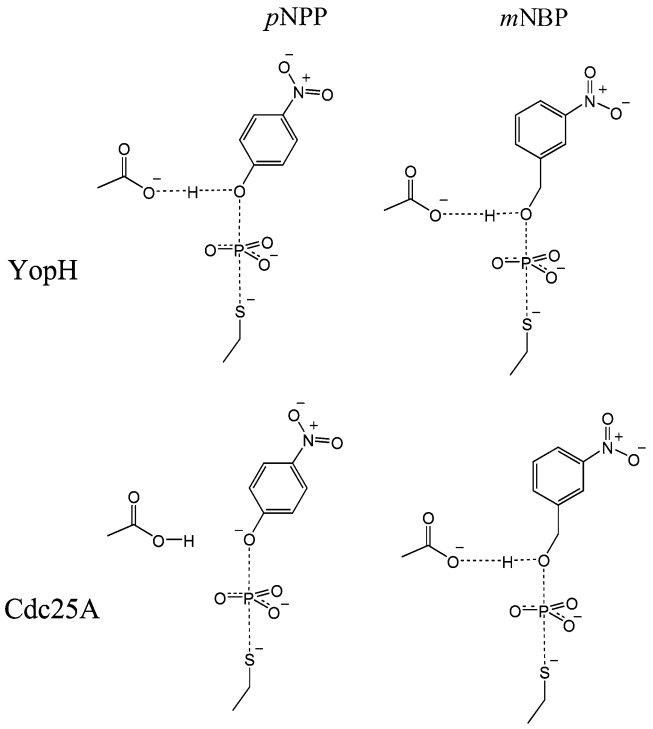

FIGURE 4: Comparison of transition state structures for YopH and Cdc25A with *p*NPP and *m*NBP as substrates.

The difference in transition states in the hydrolysis of *p*NPP and *m*NBP by YopH parallels that in the nonenzymatic hydrolysis of the monoanions of these compounds (*9*). This provides further evidence that these enzymes do not change the transition state, but simply stabilize it. This work represents an important first step in characterizing the transition state of phosphatase enzymes in hydrolyzing a less reactive more physiologically relevant substrate. In addition, it provides an important example of how the timing of enzymatic general acid catalysis might change in response to substrates with differing reactivities.

REFERENCES

1. Lad, C., Williams, N. H., and Wolfenden, R. (2003) The rate of hydrolysis of phosphomonoester dianions and the exceptional catalytic proficiencies of protein and inositol phosphatases, *Proc. Natl. Acad. Sci. U.S.A. 100*, 5607−5610.
2. Zhang, Z.-Y. (2003) Mechanistic studies on protein tyrosine phosphatases, *Prog. Nucleic Acid Res. Mol. Biol. 73*, 171−220.
3. Hengge, A. C., Sowa, G., Wu, L., and Zhang, Z.-Y. (1995) Nature of the transition state of the protein-tyrosine phosphatase-catalyzed reaction, *Biochemistry 34*, 13982−13987.
4. Hengge, A. C., Denu, J. M., and Dixon, J. E. (1996) Transition-state structures for the native dual-specific phosphatase VHR and D92N and S131A mutants. Contributions to the driving force for catalysis, *Biochemistry 35*, 7084−7092.

5. Hengge, A. C., Zhao, Y., Wu, L., and Zhang, Z.-Y. (1997) Examination of the transition state of the low-molecular mass tyrosine phosphatase 1. Comparisons with other protein phosphatases, *Biochemistry 36*, 7928−7936.
6. Rigas, J. D., Hoff, R. H., Rice, A. E., Hengge, A. C., and Denu, J. M. (2001) Transition state analysis and requirement of Asp-262 general acid/base catalyst for full activation of dual-specificity phosphatase MKP3 by extracellular regulated kinase, *Biochemistry 40*, 4398−4406.
7. McCain, D. F., Catrina, I. E., Hengge, A. C., and Zhang, Z.-Y. (2002) The catalytic mechanism of Cdc25A phosphatase, *J. Biol. Chem. 277*, 11190−11200.
8. Kirby, A. J., and Varvoglis, A. G. (1967) The reactivity of phosphate esters. monoester hydrolysis, *J. Am. Chem. Soc. 89*, 415−423.
9. Grzyska, P. K., Czyryca, P. G., Purcell, J., and Hengge, A. C. (2003) Transition state differences in hydrolysis reactions of alkyl versus aryl phosphate monoester monoanions, *J. Am. Chem. Soc. 125*, 13106−13111.
10. Zhang, Z.-Y. (1995) Are protein-tyrosine phosphatases specific for phosphotyrosine? *J. Biol. Chem. 270*, 16052−16055.
11. Zhang, Z.-Y., Wu, L., and Chen, L. (1995) Transition state and rate-limiting step of the reaction catalyzed by the human dual specificity phosphatase, VHR, *Biochemistry 34*, 16088−16096.
12. Liang, F., Huang, Z., Lee, S.-Y., Liang, J., Ivanov, M. I., Alonso, A., Bliska, J. B., Lawrence, D. S., Mustelin, T., and Zhang, Z.-Y. (2003) Aurintricarboxylic acid blocks *in vitro* and *in vivo* activity of YopH, an essential virulent factor of *Yersinia pestis*, the agent of plague, *J. Biol. Chem. 278*, 41734−41741.
13. Zhang, Z.-Y., Wang, Y., and Dixon, J. E. (1994) Dissecting the catalytic mechanism of protein tyrosine phosphatases, *Proc. Natl. Acad. Sci. U.S.A. 91*, 1624−1627.
14. Zhang, Z.-Y., Malachowski, W. P., Van Etten, R. L., and Dixon, J. E. (1994) The nature of the rate-determining steps of the *Yersinia* protein tyrosine phosphatase-catalyzed reactions, *J. Biol. Chem. 269*, 8140−8145.
15. Zhang, Z.-Y., Clemens, J. C., Schubert, H. L., Stuckey, J. A., Fischer, M. W. F., Hume, D. M., Saper, M. A., and Dixon, J. E. (1992) Expression, purification, and physicochemical characterization of a recombinant *Yersinia* protein tyrosine phosphatase, *J. Biol. Chem. 267*, 23759−23766.
16. Black, M. J., and Jones, M. E. (1983) Inorganic phosphate determination in the presence of a labile organic phosphate: assay for carbamyl phosphate phosphatase activity, *Anal. Biochem. 135*, 233−238.
17. Hengge, A. C. (2002) Isotope effects in the study of phosphoryl and sulfuryl transfer reactions, *Acc. Chem. Res. 35*, 105−112.
18. Guan, K. L., and Dixon, J. E. (1991) Evidence for protein-tyrosine phosphatase catalysis proceeding via a cysteine-phosphate intermediate, *J. Biol. Chem. 266*, 17026−17030.
19. Cho, H., Krishnaraj, R., Kitas, E., Bannwarth, W., Walsh, C. T., and Anderson, K. S. (1992) Isolation and structural elucidation of a novel phosphocysteine intermediate in the LAR protein tyrosine phosphatase enzymatic pathway, *J. Am. Chem. Soc. 114*, 7296−7298.
20. Denu, J. M., Zhou, G., Guo, Y., and Dixon, J. E. (1995) The catalytic role of aspartic acid-92 in a human dual-specific protein-tyrosine-phosphatase, *Biochemistry 34*, 3396−3403.
21. Zhang, Z.-Y., Wang, Y., Wu, L., Fauman, E., Stuckey, J. A., Schubert, H. L., Saper, M. A., and Dixon, J. E. (1994) The Cys-$(X)_5$Arg catalytic motif in phosphoester hydrolysis, *Biochemistry 33*, 15266−15270.
22. Zhang, Y.-L., Hollfelder, F., Gordon, S. J., Chen, L., Keng, Y.-F., Wu, L., Herschlag, D., and Zhang, Z.-Y. (1999) Impaired transition state complementarity in the hydrolysis of *O*-arylphosphorothioates by protein-tyrosine phosphatases, *Biochemistry 38*, 12111−12123.
23. Hoff, R. H., Wu, L., Zhou, B., Zhang, Z.-Y., and Hengge, A. C. (1999) Does positive charge at the active site of a phosphatase cause a change in mechanism? The effect of the conserved arginine on the transition state for enzymatic phosphoryl transfer in the protein-tyrosine phosphatase from *Yersinia*, *J. Am. Chem. Soc. 121*, 9514−9521.
24. Sowa, G. A., Hengge, A. C., and Cleland, W. W. (1997) ^{18}O isotope effects support a concerted mechanism for ribonuclease A, *J. Am. Chem. Soc. 119*, 2319−2320.
25. Chen, W., Wilborn, M., and Rudolph, J. (2000) Dual-specific Cdc25B phosphatase: in search of the catalytic acid, *Biochemistry 39*, 10781−10789.
26. Dunn, D., Chen, L., Lawrence, D. S., and Zhang, Z.-Y. (1996) The active-site specificity of the *Yersinia* protein-tyrosine phosphatase, *J. Biol. Chem. 271*, 168−173.
27. Zhang, Z.-Y. (1995) Kinetic and mechanistic characterization of a mammalian protein tyrosine phosphatase, PTP1, *J. Biol. Chem. 270*, 11199−11204.
28. Alhambra, C., Wu, L., Zhang, Z.-Y., and Gao, J. (1998) Walden-inversion enforced transition state stabilization in a protein tyrosine phosphatase, *J. Am. Chem. Soc. 120*, 3858−3866.
29. Czyryca, P. G., and Hengge, A. C. (2001) The mechanism of the phosphoryl transfer catalyzed by *Yersinia* protein-tyrosine phosphatase: a computational and isotope effect study, *Biochim. Biophys. Acta 1547*, 245−253.
30. Zhao, Y., Wu, L., Noh, S. J., Guan, K.-L., and Zhang, Z.-Y. (1998) Altering the nucleophile specificity of a protein-tyrosine phosphatase-catalyzed reaction: probing the function of the invariant glutamine residues, *J. Biol. Chem. 273*, 5484−5492.
31. Hoff, R. H., Hengge, A. C., Wu, L., Keng, Y.-F., and Zhang, Z.-Y. (2000) The Effects on General Acid Catalysis from Mutations of the Invariant Tryptophan and Arginine Residues in the Protein-Tyrosine Phosphatase from *Yersinia*, *Biochemistry 39*, 46−54.
32. Cleland, W. W., and Hengge, A. C. (1995) Mechanisms of phosphoryl and acyl transfer, *FASEB J. 9*, 1585−1594.
33. Hengge, A. C., Edens, W. A., and Elsing, H. (1994) Transition-state structures for phosphoryl-transfer reactions of *p*-nitrophenyl phosphate, *J. Am. Chem. Soc. 116*, 5045−5049.
34. Knight, W. B., Weiss, P. M., and Cleland, W. W. (1986) Determination of equilibrium ^{18}O isotope effects on the deprotonation of phosphate and phosphate esters and the anomeric effect on deprotonation of glucose-6-phosphate, *J. Am. Chem. Soc. 108*, 2759−2761.
35. Rudolph, J. (2002) Catalytic mechanism of Cdc25, *Biochemistry 41*, 14613−14623.
36. Benkovic, S. J., and Schray, K. J. (1978) The mechanism of phosphoryl transfer, in *Transition States of Biochemical Processes* (Gandour, R. D., and Schowen, R. L., Eds.) pp 493−527, Plenum Press, New York.
37. Thatcher, G. R. J., and Kluger, R. (1989) Mechanism and catalysis of nucleophilic substitution in phosphate esters, *Adv. Phys. Org. Chem. 25*, 99−265.
38. Hengge, A. C., and Hess, R. A. (1994) Concerted or stepwise mechanisms for acyl transfer reactions of *p*-nitrophenyl acetate? Transition state structures from isotope effects, *J. Am. Chem. Soc. 116*, 11256−11263.

BI0496182